Available online at www.sciencedirect.com
SCIENCE DIRECT®
Journal of Photochemistry and Photobiology A: Chemistry 170 (2005) 225–232
Journal of Photochemistry and Photobiology A:Chemistry
www.elsevier.com/locate/jphotochem

Photodegradation of a textile dye catalyzed by sol–gel derived nanocrystalline TiO_2 via ultrasonic irradiation

S. Senthilkumaar[a,*], K. Porkodi[a], R. Vidyalakshmi[b]

[a] *Department of Chemistry, Faculty of Engineering, PSG College of Technology, Coimbatore 641004, India*
[b] *Department of Chemistry, PSG College of Arts and Science, Coimbatore 641014, India*

Received 18 March 2004; received in revised form 23 June 2004; accepted 6 July 2004
Available online 2 October 2004

Abstract

Nanocrstalline pure anatase titania were prepared by sol–gel process at room temperature followed by ultrasonication (Ti–US). The photocatalytic activity of Ti–US has been evaluated by the degradation of textile dye, Methylene Blue in presence and absence of common inorganic salts (NO_3^-, $C_2O_4^{2-}$, SO_4^{2-}, citrate). It was observed that, in presence of anions, the degradation of the dye increases significantly. The influence of the presence of H_2O_2 on the degradation rate was studied. The dependence of photodegradation of the dye rates on various parameters such as dye concentration, photocatalyst concentration and pH were also investigated. The photodegradation rate follows first order kinetics. H_2O_2 and UV light have a negligible effect in absence of Ti–US catalyst. The relative photonic efficiency of the system is reported using phenol as a standard organic compound.
© 2004 Elsevier B.V. All rights reserved.

Keywords: Nanacrystalline TiO_2; Ultrasonication; Methylene blue-photodegradation; Inorganic anions

---

1. Introduction

Dyestuffs are important class of synthetic organic pigments, which represent an increasing environmental problem. With in the overall category of dye stuffs, methylene blue is one of the most important basic dye, used in different applications such as dyeing and printing industries. The release of this colored wastewater in the eco-system is a dramatic source of aesthetic pollution, eutrophication and perturbation in aquatic systems [1]. The available physical, chemical and biological methods are available for the treatment of textile wastewater is cost effective. However, it has been reported that most of the dyes are adsorbed on the adsorbent and are not degraded. Hence, physical, chemical and biological methods are not cost effective to Indian context. This leads to search for highly effective method to degrade the dyes into environmentally compatible products. It has been revealed from the literature that photocatalysis can be used to destroy the dyes using semiconductor catalyst under light irradiation [2–5].

Among the semiconductors used, TiO_2 is considered particularly efficient owing to the formation of electron-hole pair under illumination with near UV light. Nevertheless, the recombination of electron-hole inhibit the photocatalytic reaction process. Many researchers have reported that TiO_2 and ZnO are two most active catalyst in the degradation of dyes, pesticides, phenols, etc. [6–10].

The efficiency of titania is influenced by several factors such as crystallinity of the anatase phase [11,12], particle size, surface area [13,14] and the method of preparation [15,16]. It is known that the transformation from amorphous to anatase or rutile phase is influenced by the preparative experimental conditions [17]. Different preparation methods such as hydrolysis, sol–gel, micro emulsion or reverse miscelles, hydrothermal and mechno chemical method [18] are reported by several researchers [19–25] to synthesize nanoparticles of titania. The ultrasonication technique is extensively used for

---

[*] Corresponding author. Tel.: +9894155051; fax: +91 4222573833.
E-mail address: sspsgrp@yahoo.com (S. Senthilkumaar).

1010-6030/$ – see front matter © 2004 Elsevier B.V. All rights reserved.
doi:10.1016/j.jphotochem.2004.07.005

the preparation of mesoporous titania [26], anatase and rutile titania [27] and brookite titania [28], titania nanotubes [29] ZnO nanocrystals [30], MCM–41 silica [31]. Anatase and rutile phases are prepared to study the surface area and pH dependent surface structures of TiO_2 powders suspended in aqueous $AgNO_3$ solution is also reported [32].

In this present work, we report on the novelty of ultrasonication technique coupled with sol–gel method for the synthesis of nanocrystalline single phase pure anatase titania (Ti–US) at room temperature while others have reported mixed phases [20,27]. The influence of this irradiated photocatalyst in the degradation of MB in aqueous system was reported. Its structure is presented in Fig. 1. The parameters studied include irradiation time, effect of initial MB concentration, concentration of nanocrystalline Ti–US, effect of H_2O_2, effect of common inorganic salts and pH.

2. Materials and methods

2.1. Chemicals

Titanium (IV) *n*-butoxide (99%) purchased from Lancaster and used as such. Analar grade glacial acetic acid and *n*-butanol were obtained from Sd's fine chemicals and were triply distilled. The analar quality sodium salt of NO_3^-, SO_4^{2-}, $C_2O_4^{2-}$, Citrate, H_2O_2 (100 volumes) and dye methylene blue (MB) were procured from Sd's fine chemicals and used as received.

2.2. Synthesis of nanocryatalline TiO_2

The experimental flow chart for the synthesis of TiO_2 bulk was given in Fig. 2. Detailed procedure for the preparation of TiO_2 is discussed as follows: titanium (IV) *n*-butoxide (3.5 g) is added to 4 g of glacial acetic acid with constant stirring. To the reaction mixture, *n*-butanol (42.5 g) is added slowly. The total volume of the reactants is maintained to be 50 ml. The contents are stirred vigorously for 6–8 h. The excess solvent is evaporated by drying in a vacuum air oven at 150 °C for 12 h. The TiO_2 sol obtained was ultrasonically treated for 30 min. The derived gel is subjected to calcination at 500 °C for 30 min and labeled Ti–US. The final product is ground to get fine particles. In case of titanium alkoxide precursors, dilute solutions of the reactants, i.e., water (hydroxyl group precursor) and alkoxide (titanium precursor) in excess ethanol allow physical separation of the reactants. But titanium butoxide is extremely water sensitive precursor. Therefore, the maximum titania loading that can be achieved without second phase precipitation of titania is limited. In general, as the loading of the dispersed phase is increased, we can see the precipitation of a second phase [33].

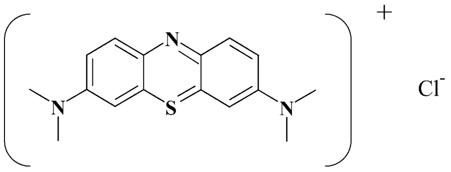

Fig. 1. Structure of methylene blue.

2.3. Photocatalytic decomposition of methylene blue

Experiments were performed in a open thermostated pyrex reactor of 250 ml capacity and provided with water circulation arrangement in order to maintain the temperature. The suspensions in the reactor were left for 60 min in dark in order to achieve the maximum adsorption of the dye on to Ti–US surface. The irradiation was carried out using 125 W (311 nm) medium pressure Hg arc lamp. The average light intensity on the reaction vessel at a distance of 15 cm from the lamp was found to be 1.6×10^{-4} Einstein min^{-1}.

In all studies, 200 ml of MB solution contain an appropriate amount of Ti–US was magnetically stirred, before and during illumination. At specific time intervals, 5 ml of the sample was withdrawn and filtered through 0.45 μm filters. Changes in the concentration of MB were observed from its characteristic absorption at 666 nm using a UV–vis spectrophotometer (Schimadzu UV-1601). The influences of

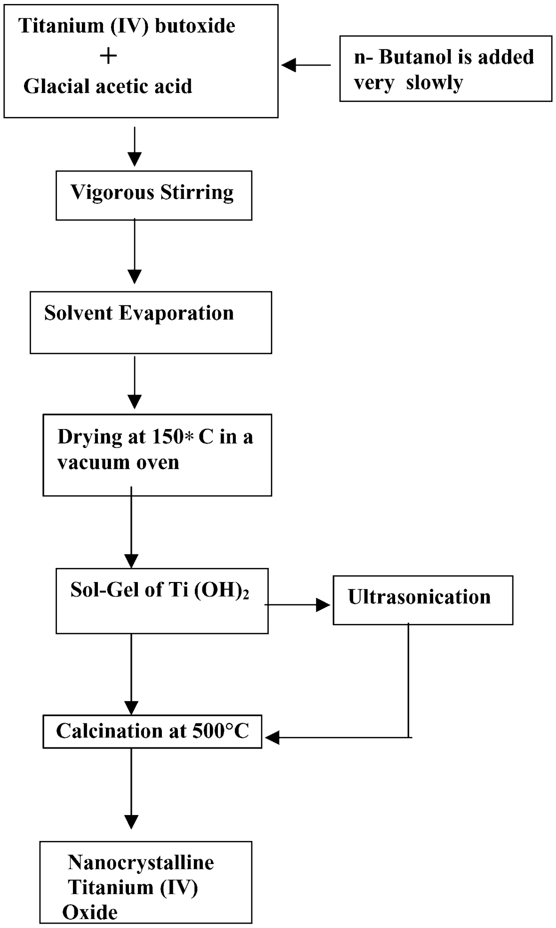

Fig. 2. Synthesis of nanocrystalline TiO_2.

(0.025 M) anions such as nitrate, oxalate, sulphate and citrate on the photodegradation of MB (10 mg/l) in presence of Ti–US (250 mg/l) at pH (6.80) were studied. All experiments, except were otherwise mentioned in the text, were carried out at natural pH (6.80).

3. Results and discussion

3.1. Characterization of photocatalyst

The XRD patterns were recorded on Schimadzu X-Ray diffractometer over a 2θ range of 20–80° with a step size of 0.02° and a collection time of 0.3 s. ($\lambda = 1.541$). The spectra were plotted and compared with data from Joint Committee Powder Diffraction Standards (JCPDS) for analysis. The crystallite size of Ti–US was calculated using Debye–Scherrer Eq. (1),

$$t = \frac{K\lambda}{B\cos\theta} \tag{1}$$

where the number $K = 0.9$ is a coefficient, $\lambda = 1.541$ Å is the X-Ray wavelength, B is the full width half maximum (FWHM) of the catalyst, θ is the diffracting angle. Specific surface area of the sample was calculated from the formula [34],

$$S = \frac{6 \times 10^3}{\rho L} \tag{2}$$

where S is the specific surface area ($m^2\,g^{-1}$), L is the average crystallite size, ρ is the density of the titania. (3.9 gcm^3) [34]. The crystallite size and surface area calculated from XRD patterns from Eqs. (1) and (2) were 12 nm and 128.21 $m^2\,g^{-1}$.

3.2. Adsorption isotherm

Adsorption tests in dark conditions were carried out in order to evaluate the equilibrium constants of the adsorption of dye on the TiO_2 surface at different concentration. The extent of equilibrium adsorption was determined from the decrease in dye concentration. The amount of dye molecules adsorbed on Ti–US was determined through Eq. (3),

$$n = \frac{V\Delta C}{W} \tag{3}$$

where n is the number of dye molecules adsorbed per gram of Ti–US, ΔC the decrease in the dye concentration in mg/l, W the weight of Ti–US in grams and V the volume of dye solution in litre. The value of $n_{\max}$ for the equilibrium of adsorption of MB was calculated as 1.7584 mg/g from the following Eq. (4),

$$\frac{C_{\mathrm{eq}}}{n} = \frac{1}{Kn_{max}} + \frac{C_{\mathrm{eq}}}{n_{max}} \tag{4}$$

where n is the number of adsorption sites on Ti–US, C_{eq} is the equilibrium concentration of dye and K is the equilibrium constant for MB adsorption [35].

3.3. Change of absorption spectra

Fig. 3 shows the change in absorption spectrum of 10 ppm MB on irradiation in an aqueous solution containing 0.125 mg/l Ti–US. The absorption spectra is seen to decrease in intensity with increase in irradiation time. The rapid decrease in the intensity of 666 nm band in Fig. 3 suggests that the chromophore responsible for characteristic color of the MB is breaking down. Since there is a linear correlation between the initial concentrations of dye at 666 nm, during the experimental procedure the photodecomposition occurs at this wavelength.

3.4. The effect of initial MB concentration and irradiation time

Fig. 4 shows the normalized concentration versus irradiation time for different initial MB concentration at fixed Ti–US concentration. It is seen from Fig. 4, a very small decrease in the concentration of MB was observed in absence of light. The additional decreases in concentration are caused by subsequent light illumination of the suspensions.

The experimental kinetic data follows the first order kinetic expression,

$$\log[C_t] = -kt + \log[C_0] \tag{5}$$

where $[C_0]$ and $[C_t]$ represent the concentration of the substrate in solution at time zero and time t of illumination respectively, and k represent the apparent rate constant (min^{-1}).

The straight line plots of log C versus t suggest the applicability of first order kinetics with respect to MB (Fig. 5). The first order rate constants were found to be 4.85×10^{-3}, 3.9×10^{-3} and 1.987×10^{-3} for dye concentrations 2, 6 and 8 mg/l, respectively. It is observed that the rate constant increases with increase in initial concentration of the dye. Similar observation was also reported by Neppolian et al.

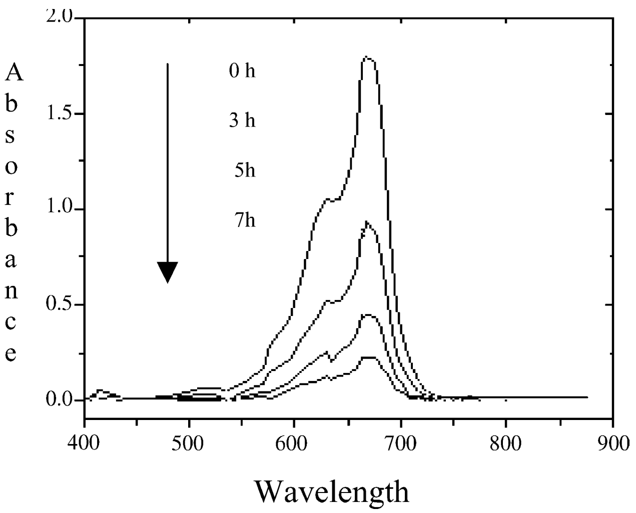

Fig. 3. Change of absorption spectra of MB with irradiation time.

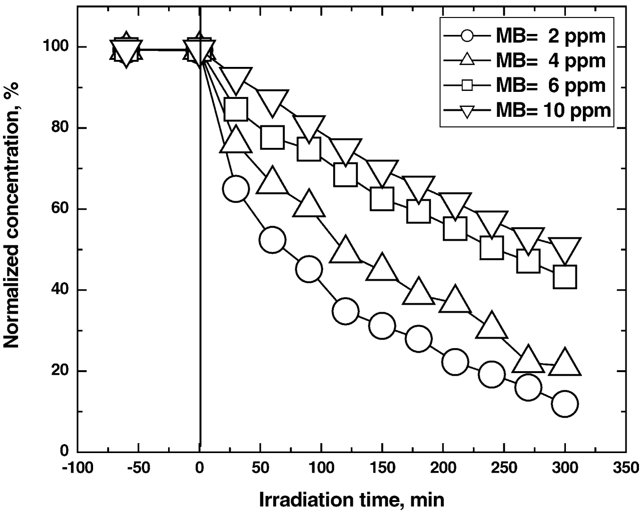

Fig. 4. Effect of initial concentration and irradiation time on MB degradation. Conditions: [Ti–US] = 0.125 mg/l; pH = 6.80.

[3–5]. Further, Davis et al. [36] and Mathew [37] explained this behavior that the path length of the photons entering the solution decreases and in low concentration the reverse effect has observed, there by increasing the number of photon absorption by the catalyst in low concentration.

Mengyue et al. [38] suggests that as the initial concentration of the dye increases, the amount of catalyst required for the degradation also increases. Since irradiation time and the amount of catalyst are constant, the OH$^{\bullet}$ (primary oxidant) formed at the surface of the catalyst is also constant. So the relative number of free radicals attacking the dye molecule increases with the amount of catalyst [39]. Hence, at higher concentration the degradation decreases with increase in the concentration of dye.

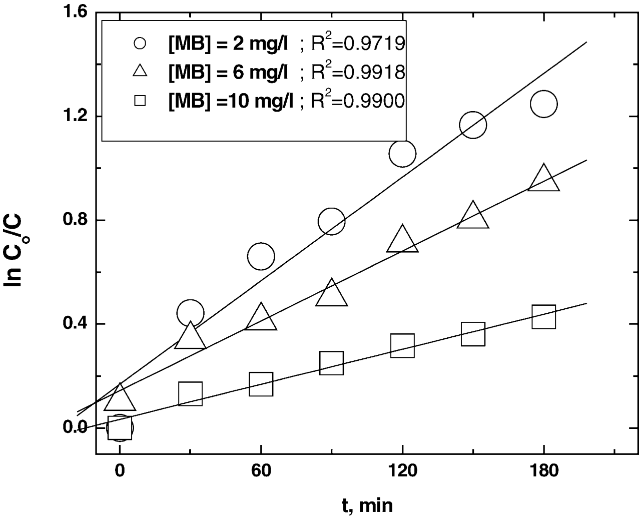

Fig. 5. Kinetics of photocatalytic MB degradation. Conditions: [Ti–US] = 0.125 mg/l; pH = 6.80.

3.5. *Effect of catalyst concentration*

Experiments were carried out with different concentrations of catalyst (0.125–0.750 g/l) at fixed MB concentration (10 mg/l). It has been observed that the initial rate increases with an increase in the amount of catalyst and that it remains almost constant above a certain level and is presented in Table 1. This has been explained as the concentration of the catalyst is increased; the number of photons absorbed and the number of dye molecules adsorbed are increased with respect to an increase in the number of catalyst molecules. The density of the molecule in the area of illumination also increases and thus the rate gets enhanced. After a certain level, the dye molecules available are not sufficient for adsorption by the increased number of catalyst molecule. Hence, the additional catalyst powder is not involved in the photocatalytic activity and the rate does not increased with increase in the amount of catalyst beyond certain limit. It is also expected that the aggregation of the catalyst molecules at high concentration must also be considered, which causes the decrease in the number of active surface sites. The experimental data are found in good agreement with those reported by Sauer et al. [40] for the degradation of Safira dye using Degussa P-25. Neppolian et al. [6] also reported the decreased per cent degradation of reactive dyes at higher catalyst concentration. Further, it is explained that the deactivation of activated molecule by collision with the ground state molecule with the shielding of TiO_2 may also take place according to Eq. (6),

$$\text{Ti–US}^{*} + \text{Ti–US} \rightarrow \text{Ti–US}^{\bullet} + \text{Ti–US} \qquad (6)$$

where Ti–US* is the Ti–US with active species adsorbed in its surface and Ti–US$^{\bullet}$ the deactivated form of Ti–US. Hence, an optimum catalyst concentration has to be maintained to ensure total absorption of photons for efficient photodegradation [41].

Galindo et al. [42] reported an empirical initial degradation rate and catalyst concentration as $r^0 \propto [TiO_2]^n$ [dye], where n is the exponent less than one for the dye studied in reaction to the lower concentration of catalyst. In our present work, the initial degradation rate follows a similar relationship and the 'n' value was found to be 0.61 when the Ti–US concentration was less than 1 g/l (Fig. 6).

Table 1
Effect of Ti–US concentration on the decolorization rate

$[TiO_2]$ (g/l)	r_o (mg/l min)
0.125	0.0183
0.250	0.0328
0.375	0.0387
0.500	0.0417
0.625	0.0408
0.750	0.0396

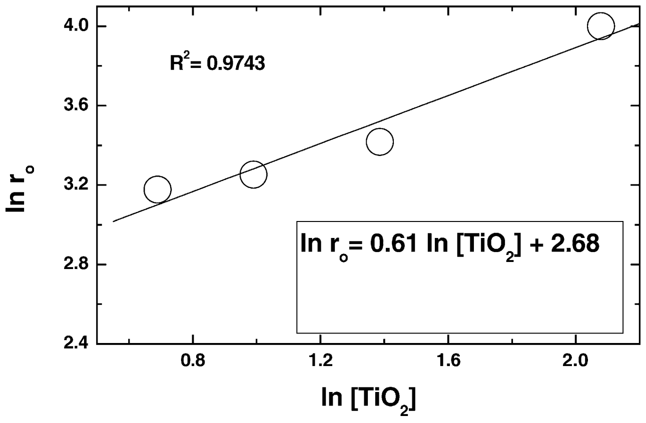

Fig. 6. Effect of catalyst concentration on MB degradation rate. Conditions: [MB] = 10 mg/l; pH = 6.80.

3.6. *Effect of pH*

The influence of pH on the decolorization of MB is shown in Fig. 7. The results showed that, there was a strong dependence of pH of the solution on the heterogeneous photo process. It is known that the metal oxide particles suspended in water behave similar to diprotic acids. For TiO_2, hydroxyl groups undergo two acid base equilibria:

$$>TiOH_2^+ \leftrightarrow >TiOH + H^+$$

$$>TiOH \leftrightarrow >TiO^- + H^+$$

Generally, for charged substrates, a significant dependency of the photocatalytic degradation efficiency on pH value had been observed, since the overall surface charge and hence the adsorptive properties of TiO_2 particles depend strongly on solution pH [43,44].

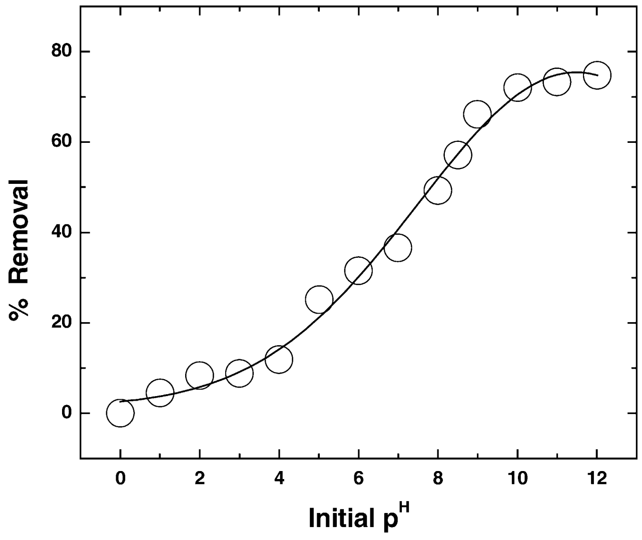

Fig. 7. Effect of initial pH on MB degradation. Conditions: [MB] = 10 mg/l; [Ti–US] = 0.125 mg/l; Irradiation time = 4 h.

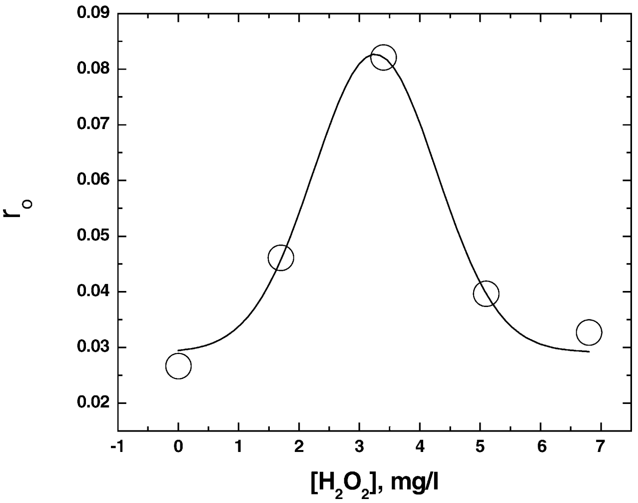

Fig. 8. Effect of H_2O_2 on MB degradation. Conditions: [MB] = 10 mg/l; [Ti–US] = 0.125 mg/l; pH = 10.0.

In our experiments, any changes in initial degradation rate with varying pH values must be ascribed to variations of the acid/base properties of the Ti–US particle surface (Eq. (7) and (8). Since the phototoxidation of dyes is accompanied by the release of protons [45], its efficiency may then change because of the reversible protonation of the Ti–US surface. The MB is a cationic dye in aqueous solution. In acidic pH range ($pH < 5.0$) Ti–US acquire positive charge and hence electrostatic repulsion between Ti–US and dye cation retards the degradation rate. On the other hand, in basic pH ($pH > 5.0$), electrostatic interaction between the negative Ti–US and dye cation lead to strong adsorption with the corresponding high rate of degradation and reached a maximum at pH 10. This behaviour is characteristics for many photocatalytic systems and similar results have been reported by the photodegradation of other dyes [45].

3.7. *Effect of H_2O_2 on the photodegradation of MB*

Experiments were conducted to evaluate the effect of H_2O_2 on the MB photodegradation (Fig. 8). In our study, photocatalytic efficiency increases as the concentration of H_2O_2 increases and reaches optimum at 3.4 mg/l and further increase in concentration up to 6.8 mg/l leads to decrease in the photodegradation rate. The addition of H_2O_2 increases the concentration of $OH^\bullet$ radical since it inhibit the e^-, h^+ recombination according to the Eq. (9),

$$TiO_{2(e^-)} + H_2O_2 \rightarrow TiO_2 + OH^- + OH^\bullet \qquad (9)$$

H_2O_2 is considered to have two functions in the photocatalytic degradation. It accepts a photogenerated conduction band electron thus promotes the charge separation (Eq. (10)) and it also forms $OH^\bullet$ (Eq. (11)).

$$H_2O_2 + e^- \rightarrow OH^- + OH^\bullet \qquad (10)$$

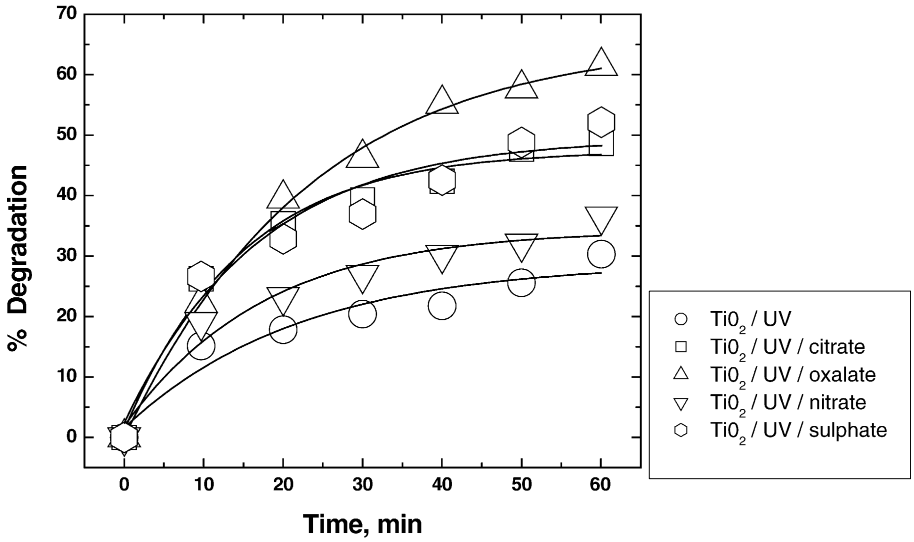

Fig. 9. Effect of common inorganic salts on MB degradation. Conditions: [MB] = 10 mg/l; [inorganic salt] = 250 mg/l]; [Ti–US] = 0.250 mg/l; pH = 6.80.

$$H_2O_2 + O_2^{\bullet -} \rightarrow OH^- + OH^\bullet + O_2 \qquad (11)$$

The addition of H_2O_2 is a well known mechanism to increase the rate of photocatalytic degradation with higher quantum yield of formation of $OH^\bullet$ [46,47]. Consequently, the degradation rate is expected to increase. Further increase of H_2O_2 after the quantum level, decrease the rate of degradation slowly. This negative effect of high concentration of H_2O_2 may be due to the formation of $OH_2^\bullet$. When the H_2O_2 concentration is higher, $OH_2^\bullet$ formed is significantly less reactive than $OH^\bullet$. Wang and Hong [48] reported that the H_2O_2 on the catalyst surface acts as a powerful $OH^\bullet$ scavenger (Eqs. (12) and (13)) along with a photogenerated holes (Eq. (14)) and thus inhibit the generation of $OH^\bullet$ radical and thereby decrease the degradation rate.

$$H_2O_2 + OH^\bullet \rightarrow H_2O + HO_2^\bullet \qquad (12)$$

$$HO_2^\bullet + OH^\bullet \rightarrow H_2O + O_2 \qquad (13)$$

$$H_2O_2 + h_{vb}^+ \rightarrow HO_2^\bullet + H^+ \qquad (14)$$

Several researchers have reported the beneficial effect of H_2O_2 on the photocatalytic degradation of pesticides [49,50], benzene, organo phosphorous derivatives, organo halides and dioxins [51,52], whereas, a negative effect have also been reported by Chemsedine and Bohem [53] for the degradation of chloro acid on TiO_2.

3.8. Effect of Inorganic salts

The effect of inorganic salts on the degradation process was investigated with common inorganic salts such as nitrate, sulphate, citrate and oxalates (0.025 M). As can be seen from the Fig. 9, the effectiveness of Ti–US/UV system was significantly increased. The order of reactivity towards the decomposition of MB was found to be oxalate > sulphate > citrate > nitrate. Adsorption of MB on TiO_2 was significantly increased in presence of anion species. It can be explained as the reaction of the positive hole (h^+) formed on the Ti–US with anions and those anions behave like h^+ scavengers resulting prolonged color removal in 0–30 min irradiation. Probably, the adsorbed anions compete with the dye for the photooxiding species on the surface to form oxidizing inorganic radicals. It is expected that the recombination of h^+ and the electron will be prohibited by these anions leaving the electron for the photodecomposition of MB. It is also expected that some of these radical anions react with the chromophoric groups of surface adsorbed dye, may enhance the rate of degradation. The observed effect is still thought to be strong adsorption of anions on Ti–US surface [54,55].

3.9. Calculation of relative photonic efficiency

In order to compare the degradation and efficiency of Ti–US, the relative photonic efficiency (ξr) was calculated using Eq. (15).

$$\xi r = \frac{\text{Rate of disappearance of dye}}{\text{Rate of disappearance of phenol}} \qquad (15)$$

where both (initial) rates are obtained under exactly the same condition. The relative photonic efficiency of the dye degradation is 1.06. The efficiency is greater than unity, indicating that the initial photocatalysed oxidative degradation of the dye is more efficient than for phenol [56].

4. Conclusions

- Nanocrystalline, pure anatase titania (Ti–US) were prepared by sol–gel process via ultrasonic irradiation.
- The average crystallite size calculated from Debye–Scherrer equation was found to be 12 nm.
- From the XRD data, the surface area of Ti–US were calculated and found to be 128.2 m^2/g.
- It was observed that Ti–US is efficient for the degradation of MB from aqueous solution.
- From the experimental results, the dependence of the Ti–US concentration on the initial decolorization rate follows a relationship, $r^0 \propto [TiO_2]^n$. The value of n was found to be 0.61.
- The photocatalytic rate of MB increased in presence of H_2O_2.
- The influence of H_2O_2 on the decomposition rate reveals the fact that the most possible oxidation mechanism of MB is the dual hole–radical mechanism.
- The optimum concentration of 3.4 mg/l of H_2O_2 is required for the effective degradation of 10 mg/l of MB at pH 10. However, at higher concentration the H_2O_2 would quench the $OH^{\bullet}$ and decrease the rate of the reaction.
- The experimental data suggests the degradation of MB follows first order kinetics.
- The sol–gel coupled with ultrasonic technique is a fast and gives uniform distribution of crystallites of pure anatase with average crystallite size of 12 nm.
- Ultrasonication does not only reduce the crystallite size but also enhances the hydrolysis of titanium alkoxide for faster and better crystallization of anatase nanoparticles.
- From the result of present work and the literature, one could understand that photocatalytic treatment of textile industry wastewater as a promising tool for the decolorization of colored wastewaters.

Acknowledgements

The authors are thankful to Dr. R. Subramanian, Department of Metallurgy for XRD analysis.

References

[1] J.-M. Herrmann, M. Vautier, C. Guillard, J. Catal. 201 (2001) 46.
[2] M.R. Hoffmann, S.T. Martin, W. Choi, D.W. Bahnemann, Chem. Rev. 95 (1995) 69.
[3] B. Neppolian, S. Sakthivel, M. Palanichamy, B. Arabindoo, V. Murugasen, Stud. Surf. Sci. Catal. 113 (1998) 329.
[4] B. Neppolian, S. Sakthivel, M. Palanichamy, B. Arabindoo, V. Murugasen, J. Environ. Sci. Health A 43 (1999) 1829.
[5] B. Neppolian, S. Sakthivel, M. Palanichamy, B. Arabindoo, V. Murugasen, Bull. Cat. Soc. India 81 (1999) 164.
[6] B. Neppolian, S. Sakthivel, M. Palanichamy, B. Arabindoo, V. Murugasen, J. Hazard. Mater. B 89 (2002) 303.
[7] N. Serpone, E. Pelizzetti (Eds.), Photocatalysis: Fundamentals and Applications, Wiles, New York, 1989.
[8] I.K. Konstantinou, T.A. Albanis, Appl. Catal. B 42 (2003) 319.
[9] Vulliet Emmanuelle, Emmelin Corinne, Chovelon Jean- Marc, Guillard Chantal, Herrmann Jean Marie, Appl. Catal. B 38 (2002) 127.
[10] I. Poulios, I. Tsachpinis, J. Chem. Technol. Biotechnol. 74 (1999) 349.
[11] S.I. Nishimoto, B. Ohtani, H. Hajiwara, T. Kagiya, J. Chem. Soc. Faraday Trans. I 81 (1985) 61.
[12] M.A. Fox, M.T. Dulay, Chem. Rev. 93 (1993) 341.
[13] Z. Zhang, C.C. Wang, R. Zakaria, J.Y. Ying, J. Phys. Chem. B 102 (1998) 10871.
[14] H. Zhang, R.L. Penn, R.J. Hamers, J.F. Banfield, J. Phys. Chem. B 103 (1999) 4656.
[15] K.M. Reddy, C.V. Gopal Reddy, S.V. Manorama, J. Solid State Chem. 158 (2001) 180.
[16] C.C. Wang, J.Y. Ying, Chem. Mater. 11 (1993) 3113.
[17] P. Madhu kumar, S. Badrinarayann, M. Sastry, Thin Solid Films 358 (2000) 122.
[18] S. Yin, Q. Zhang, F. Saito, T. Sato, Chem. Lett. 32 (2003) 4.
[19] E. Vigil, J.A. Ayllon, A.M. Peiro, R.R. Clemente, Langmuir 17 (2001) 891.
[20] H. Zhang, M. Finnegan, J.F. Banfield, Nano Lett. 1 (2001) 81.
[21] E. Scolan, C. Sanchez, Chem. Mater. 10 (1998) 3217.
[22] V. Chhabra, V. Pillai, B.K. Mishra, A. Morrone, D.O. Shah, Langmuir 11 (1995) 3307.
[23] R.R. Basca, M. Gratzel, J. Am. Ceram. Soc. 79 (1996) 2185.
[24] E. Stathatos, P. Lianos, F.V. Del Monte, D. Levy, D. Tsiourvas, Langmuir 13 (1997) 4295.
[25] X.M. Wu, L. Wang, Z.C. Tan, G.H. Li, S.S. Qu, J. Solid State Chem. 156 (2001) 220.
[26] Y.Q. Wang, S.G. Chen, X.H. Tang, O. Palchik, A. Zaban, Y. Koltypin, A. Gedanken, J. Mater. Chem. 11 (2002) 521.
[27] W. Huang, X. Tang, Y. Wang, Y. Koltypin, A. Gedanken, Chem. Commun. (2000) 1415.
[28] J.C. Yu, J. Vu, W. Ho, L. Zhang, Chem. Commun. (2001) 1942.
[29] Y. Zhu, H. Li, Y. Koltypin, Y.R. Hacohen, A. Gedanken, Chem. Commun. (2001) 2616.
[30] D. Qian, J.Z. Jiang, Hansen Poul Lenvig, Chem. Commun. (2003) 1078.
[31] X. Tang, S. Liu, Y. Wang, W. Huang, E. Sominski, O. Palchik, Y. Koltypin, A. Gedankan, Chem. Commun. (2000) 2119.
[32] Y. Zhu, H. Li, C.L. Tsai, Huang, Mater. Sci. Eng. (2002) A001.
[33] A. Hanprasopwattana, T. Reiker, A.G. Sault, A.K. Datye, Catal. lr 45 (1997) 165.
[34] P.S. Awati, S.V. Awate, P.P. Shah, V. Ramaswamy, J. Photochem. Photobiol. A 4 (2003) 393.
[35] S. Parra, J. Olivero, C. Pulgarin, Appl. Catal. B 36 (2002) 75.
[36] R.J. Davis, J.L. Gainer, G.O. Neal, I. Wenwu, Water Environ. Res. 66 (1994) 50.
[37] R.W. Matthews, J. Chem. Soc., Faraday Trans. 85 (1989) 1291.
[38] Z. Mengyue, C. Shifu, T. Yaown, J. Chem. Tech. Biotechno 1 64 (1995) 339.
[39] L. Zang, C.Y. Liu, X.M. Ren, J. Photochem. Photobiol. A 85 (1995) 239.
[40] T. Sauer, G. Cesconeto Neto, H.J. Jose, R.F.P.M. Moreira, J. Photochem. Photobiol. A 149 (2002) 147.
[41] J.M. Herrmann, Catal. Today. 24 (1995) 157.
[42] G. Galindo, P. Jacques, A. Kalt, Chemosphere 45 (2001) 997.
[43] W.Z. Tang, H. An, Chemosphere 31 (1995) 4157.
[44] K. Wang, Y. Hisieh, C. Wu, C. Chang, Chemosphere 40 (2000) 389.
[45] I. Poulios, I. Tsachpinis, J. Chem. Technol. Biotechnol. 71 (1999) 349.
[46] C. Hachem, F. Bocquillon, O. Zahraa, M. Bouchy, Dyes and Pigments. 49 (2001) 117.
[47] P. Salvador, F. Decker, J. Phys. Chem. 88 (1984) 6116.
[48] Y. Wang, C.S. Hong, Wat. Res. 33 (1999) 2031.
[49] Z. Mengyne, C. Shifu, T. Yaowu, J. Chem. Technol. Biotechnol. 64 (1995) 339.

[50] D. Weichgrebe, BeitragZurChemison - Oxidation Abwasserbehandlung, Ph.D. Dissertation. TV Clausthal, Germany, 1994.
[51] E. Wolfrum, D.F. Ollis, Hydrogen peroxide in Hetrogeneous Photocatalysis, in: G. Helz, R. Zepp, D. Croby (Eds.), Aquatic and Surface Photochemistry, CRC Press, Boca Raton, FL, 1994, p. 451.
[52] K. Tanaka, T. Hisanaga, K. Harada, Photocatalysis degradation of organohalides compounds in semiconductive suspension with added hydrogen peroxide, New. J. Chem. 13 (1989) 5.
[53] A. Chemsedine, H.P. Bohem, J. Mol. Catal. 60 (1990) 295.
[54] M. Abdullah, G.K.C. Low, R.W. Mathews, J. Phys. Chem. 94 (1990) 6820.
[55] M. Bekbolet, Z. Boyacioglu, B. Ozkaraova, Water Sci. Technol. 38 (1998) 155.
[56] N. Serpone, G. Sauve, R. Koch, H. Tahiri, P. Pichat, E. Pelizzetti, H. Hidaka, J. Photochem. Photobiol. A 94 (1996) 191.